IEEE Access
Multidisciplinary | Rapid Review | Open Access Journal

Received April 14, 2019, accepted May 10, 2019, date of publication May 15, 2019, date of current version May 23, 2019.

Digital Object Identifier 10.1109/ACCESS.2019.2916798

Field-of-View and Impact Angle Constrained Guidance Law for Missiles With Time-Varying Velocities

BOJUN LIU, (Student Member, IEEE), MINGSHAN HOU, AND YAJUN LI
School of Automation, Northwestern Polytechnical University, Xi'an 710072, China
Corresponding author: Bojun Liu (bojun.liu@mail.nwpu.edu.cn)

ABSTRACT A novel nonlinear non-switching guidance strategy is proposed for missiles with time-varying velocities intercepting stationary targets, considering impact angle, seeker's field-of-view, and input saturation constraints, simultaneously. A new nonlinear control oriented mathematical model is established, and the guidance design problem is converted to be the issue of tracking control of a nonlinear system with the partial state constraint. In the first step, a bounded virtual guidance law is designed based on hyperbolic tangent function. In the second step, the effect of the input saturation is compensated with a first-order filter. Integral barrier Lyapunov function based stability analysis shows that the tracking errors of the whole guidance system converge to zero uniformly, and the prescribed guidance constraints are not violated. Finally, the numerical simulations are performed to demonstrate the effectiveness of the proposed guidance law.

INDEX TERMS Guidance law, impact angle control, field-of-view constraint, input saturation, hyperbolic tangent function, integral barrier Lyapunov function.

I. INTRODUCTION

Guidance law is indispensable for a missile to intercept a target. Proportional navigation (PN) guidance has been widely applied to tactical guided missiles because of its simplicity in implementation [1]. However, in modern warfares, many targets are clad in armor to bolster their defenses. In some guidance missions, it is necessary for a missile to select a predetermined impact angle in the terminal phase of the homing to hit the weak point of the armored target for increasing warhead effectiveness and strengthening offensive capabilities.

The issue of impact angle control guidance (IACG) has been studied intensely for a few decades. The previous works can be mainly classified into the following categories of method: optimal control approaches [2]–[9], PN based approaches [10]–[15], sliding mode control (SMC) approaches [16]–[22], backstepping control approaches [22]–[26], and other methods [27], [28]. Since imposing the impact angle control may give rise to the highly curved trajectories of missiles, the targets may be out of the seeker's maximum detection limit, especially for the missiles equipped with strapdown seekers, which have narrow angles of view. Thus, the IACG laws with seeker's field-of-view (FOV) constraint were studied in the past few years, and these works can be mainly classified into the following three methods: linear approaches [29]–[32], PN based approaches [33]–[37], and SMC approaches [38]–[40].

The guidance laws were designed as polynomial forms of time-to-go or relative range in common linear approaches [29], [30]. With linearizing the flight path angles, the closed form solutions of the lead angles of missile in these two laws were also obtained as the polynomial forms, so the maximum lead angles of missile can be modulated by adjusting guidance gains in advance. Besides, optimal control theory was involved in the IACG designs [31], [32]. The FOV constraint in these two laws were handled directly by utilizing the general optimal control method with an inequality constraint of state variable.

While the four linearized approaches mentioned above for seeker's FOV constrained IACG were all derived based on small angle hypotheses, some nonlinear guidance laws using the characteristics of the PN or biased proportional navigation (BPN) have been studied based on multi-phase guidance structure. BPNs with biased-shaping methods considering seeker's FOV and acceleration constraints were proposed in [33], [34]. In [35], a PN based switched-gain guidance

The associate editor coordinating the review of this manuscript and approving it for publication was Chaoyong Li.

strategy was developed for impact angle control. Therein, the navigation gains were determined by numerical solutions for dealing with the seeker's FOV and acceleration constraints. By the fact that the PN with $N = 1$ maintains the missile lead angle as a constant in the first stage, the switched-gain PN guidance in [36] changed the navigation gain from $N = 1$ to $N \geq 2$ to satisfy the impact angle control in the second stage. The guidance scheme in [37] was composed of modified deviated pure pursuit with the error feedback loop in the first stage to maintain the constant missile lead angle, and the PN with $N \geq 3$ in the second stage for impact angle constraint. In addition, the maximum acceleration limits were also investigated in two-phase laws [36], [37].

Except for PN based approaches, SMC theory was also used to design nonlinear FOV constrained IACG laws. A switching logic was adopted in [38], which added an additional term in the traditional terminal sliding mode IACG law when the missile lead angle tries to exceed the prescribed boundary value to maintain the seeker lock-on. In [39], the seeker's FOV limit was transformed to be the constraint of the relative velocity perpendicular to the line-of-sight (LOS) between missile and target, and this limit was not violated in both sliding phase and reaching phase by introducing a special sliding mode surface and by designing integral barrier Lyapunov function (iBLF) based reaching law. A new sliding mode surface with a magnitude-limited sigmoid function was designed in [40] to prohibit the missile lead angle from exceeding the specified limit and also for impact angle control. And this guidance law is available for bearings-only measurements since it involves no information about relative range and LOS rate.

It is seen that the FOV constrained IACG has been studied in the past few years. However, we noticed that there are still some minor problems in the existing laws, and they can be described as follows.

- Small angle hypotheses are required in the linear approaches [29]–[32]. Whereas the simulations of these laws shows that the flight path angles and lead angles of missile become large especially during the midcourses. Thus, linear approaches may reduce the guidance precision and lead to large miss distances.
- Guidance commands are discontinuous in the PN based methods [33]–[37]. Multi-phase strategies and switching logics are involved in these laws, so the commands suffer from abrupt-jumping at some unknown time. And the jumping commands may challenge the tracking performances of the missile control systems.
- Derivations and simulations of the SMC based guidance laws [38]–[40] are performed with assuming that the missiles have constant velocities. But this assumption may not hold in practice since homing missile velocities are time-varying due to thrust, drag and gravity effects.

In FOV constrained impact time control guidance law design [41], the FOV limitation was transformed to be the output constraint of a nonlinear system, and backstepping technique combined with iBLF was used in the design procedure. IBLF, proposed in [42], provided a direct way for the controller design of a state constrained nonlinear system. However, for a controllable practical dynamic system, the controller may be required to have real-time processing ability and the actuator performance may be restricted due to physical constraint, which may challenge the controller design based on iBLF to achieve state limitation, since the off-line feasibility check procedures may be involved and the freedom for control input may be required [42]–[44].

In this paper, A new nonlinear control oriented mathematical model is established for the FOV constrained IACG design. This guidance problem is converted to be the issue of tracking control of a nonlinear system with partial state constraint, which provide a method to deal with the problem from backstepping control point of view for the first time. Firstly, a bounded hyperbolic tangential virtual guidance law is designed to remove the feasibility conditions for the application of iBLF. Secondly, a time-varying first-order filter is designed to compensate the effect of commands saturation. Then iBLF based Lyapunov analysis shows the global stability of the guidance system. More importantly, compared with the existing studies about FOV constrained IACG designs, the proposed method has the following advantages:

- In the derivation of the proposed law, the three minor problems mentioned above in the existing literatures [29]–[40] are all avoided. The guidance law in this paper is nonlinear and non-switching essentially, and it is available for missiles with time-varying velocities.
- In the simulation, the missile under the proposed guidance law can achieve the impact from all rational aspects. Simulations show that the missile can intercept the target with impact angles from 0 deg to -180 deg, and this impact angle selection range is much larger than that in [29]–[40].

The remainder of this paper is organized as follows. In Section II, the mathematical model of the guidance system is established, and the multiple objectives of the guidance design are illustrated. The proposed guidance law is derived and the stability of the guidance system is analyzed in Section III. Section IV substantiates the guidance strategy via numerical simulations and Section V draws the conclusion of this paper.

II. PROBLEM FORMULATION

This section presents the dynamics of the missile-target engagement in order to establish the nonlinear mathematical model for the guidance design. As shown in Fig. 1, a two-dimensional engagement geometry between the missile M and the target T is considered in the inertial coordinate frame XOY, where r and λ denote the relative range and the LOS angle between the missile and target; V_M, γ_M and a_M denote the velocity, flight path angle and the normal acceleration of the missile, respectively; $-\gamma_d \in [-\pi, 0]$ is the desired constant impact angle; $\theta_M \in [-\pi, \pi)$ is the missile lead angle, which is defined as

$$\theta_M = \gamma_M - \lambda. \tag{1}$$

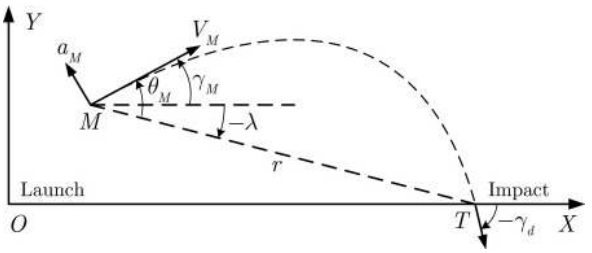

FIGURE 1. Planar engagement geometry.

All the angles mentioned above are defined as positive in the counterclockwise direction. Then the relative kinematic equations between the missile and target can be expressed as

$$\dot{r} = -V_M \cos\theta_M, \tag{2}$$
$$r\dot{\lambda} = -V_M \sin\theta_M. \tag{3}$$

The dynamics of the missile motion with time-varying velocity are given by

$$m\dot{V}_M = T - D - mg\sin\gamma_M, \tag{4}$$
$$V_M\dot{\gamma}_M = a_M - g\cos\gamma_M, \tag{5}$$

where m is the missile mass, g is the gravitational acceleration, T and D are the longitudinal thrust and aerodynamic drag force of the missile, respectively.

Since the target to be attacked is considered to be stationary in this paper, the most direct interception strategy is to regulate the velocity vector of missile to point towards the target. And this guidance scheme can be represented as $\theta_M = 0$ and $\dot{r} < 0$.

In addition, the impact angle control is equivalent to the regulation of the terminal flight path angle of missile, i.e., $\gamma_M(t_f) = -\gamma_d$, where t_f is the terminal guidance time. It can be obtained from (1) that the impact angle control can be further transformed to $\lambda = -\gamma_d$ on the basis that $\theta_M = 0$ occurs before the terminal guidance time, i.e., the homing strategy mentioned above is ensured to take effect.

Moreover, the lead angle of missile in this paper needs to be limited since it almost determines the seeker's FOV range, especially when the angle-of-attack of missile is small enough to be neglected. Therefore, the seeker's FOV constraint can be represented as $|\theta_M| < k_b < \pi/2$, where k_b is a positive constant, whose value hinges on the prescribed seeker's maximum detection angle range.

To facilitate the guidance law design, the following three assumptions can be made without loss of generality in finite guidance time.

Assumption 1: The time-varying missile velocity is bounded and always satisfies the inequality $V_M > 0$.

Assumption 2: The relative range between missile and target is bounded and always satisfies the inequality $r > 0$.

Assumption 3: The initial lead angle of missile satisfies the inequality $|\theta_M(t_0)| < k_b$, where t_0 denotes the initial guidance time.

Differentiating (1) with respect to time and substituting (5) into it yield

$$\dot{\theta}_M = \frac{a_M}{V_M} - \frac{g\cos\gamma_M}{V_M} - \dot{\lambda}. \tag{6}$$

Combining (3) and (6), and considering the input saturation, the nonlinear state equations of the guidance system are established as

$$\begin{cases} \dot{\lambda} = -\dfrac{V_M}{r} f(\theta_M)\,\theta_M, \\ \dot{\theta}_M = \dfrac{\mathrm{sat}(a_M)}{V_M} - \dfrac{g\cos\gamma_M}{V_M} - \dot{\lambda}, \end{cases} \tag{7}$$

in which

$$f(\theta_M) = \begin{cases} \dfrac{\sin(\theta_M)}{\theta_M}, & \theta_M \neq 0, \\ 1, & \theta_M = 0, \end{cases}$$
$$\mathrm{sat}(a_M) = \begin{cases} a_M \,\mathrm{sgn}(a_M), & |a_M| > a_{\max}, \\ a_M, & |a_M| \le a_{\max}, \end{cases} \tag{8}$$

where $a_{\max}$ denote the known upper bound of the guidance command a_M. Besides, the following lemma and corollary are helpful for the guidance design.

Lemma 1: The inequality $0 \le f(\theta_M) \le 1$ always holds on $\theta_M \in [-\pi, \pi)$.

Proof. It can be obtained that $f(-\pi) = 0$, and $f(\theta_M) = 1$ when $\theta_M \to 0$ by applying L'Hôpital's rule, so $f(\theta_M)$ is a continuous function on $\theta_M \in [-\pi, \pi)$. Besides, $\forall x \in (0, \pi)$, we have $\cos x < 1$, and the inequality $\int_0^x \cos y dy < \int_0^x 1 dy$, i.e., $0 < \sin x < x$ always holds. Thus, we can obtain $0 < f(\theta_M) < 1$ on $(0, \pi)$. Then this proof can be ended since $f(\theta_M)$ is an even function.

Corollary 1: The inequality $0 < f(\theta_M) \le 1$ always holds on $\theta_M \in (-k_b, k_b)$.

Proof. This corollary is easy to be obtained according to Lemma 1 and that the value of k_b, i.e., the maximum of the seeker's FOV angle range, is set less than $\pi/2$ in practice.

Now the control objectives of the nonlinear system (7) in this paper can be summarized as follows: To design the bounded guidance commands a_M to guarantee λ converging to $-\gamma_d$ for impact angle control, θ_M converging to zero and $\dot{r} < 0$ for homing constraint, and the inequality $|\theta_M| < k_b$ always holds for seeker's FOV limit.

III. GUIDANCE LAW DESIGN

In this section, the proposed guidance law is substantiated to satisfy the prescribed multiple constraints via three subsections. In Subsection III-A, hyperbolic tangent function and its two useful properties are introduced for promoting the guidance design. The details of the proposed guidance law are presented in Subsection III-B. And the analysis of the guidance system under the guidance commands is given in Subsection III-C.

A. HYPERBOLIC TANGENT FUNCTION

Hyperbolic tangent function $\tanh(x)$ is a smooth continuous function defined in $x \in \mathbb{R}$, and it is given by

$$\tanh(x) = \frac{e^x - e^{-x}}{e^x + e^{-x}}. \tag{9}$$

We noticed that hyperbolic tangent function was utilized to substitute sign function to eliminate chattering in variable structure guidance law [40], was used to design adaptive guidance law [45], and was weighted in optimal guidance strategy [46]. In this paper, this function serves the design of virtual guidance law to remove the off-line feasibility check procedure in the further utilization of iBLF. For the sake of the analysis in Subsection III-C, two properties of hyperbolic tangent function are given as follows.

Property 1: The function $x\tanh(x)$ is a positive definite function with respect to x on $x \in \mathbb{R}$.

Property 2: The inequality $|\tanh(x)| < 1$ holds on $x \in \mathbb{R}$.

Note that these two properties are easy to be obtained, and the proofs are omitted here.

B. NONLINEAR GUIDANCE LAW

Recalling the guidance system (7), the two tracking errors of the system are defined as

$$e_1 = \lambda - (-\gamma_d), \tag{10}$$
$$e_2 = \theta_M - \theta_d, \tag{11}$$

where θ_d is the virtual guidance law to be designed. Then the guidance design procedure is detailed in the following two steps.

Step 1: Differentiating (10) with respect to time and substituting (7) and (11) into it yield

$$\dot{e}_1 = -\frac{V_M}{r} f(\theta_M)(\theta_d + e_2). \tag{12}$$

Now the virtual guidance law θ_d is selected as

$$\theta_d = k_a \tanh(c_1 e_1), \tag{13}$$

where $k_a = k_b - \varepsilon > 0$, c_1 and ε are two positive constants.

Using (10) results in the time derivative of the virtual guidance law as

$$\dot{\theta}_d = c_1 k_a \dot{\lambda}\left(1 - \tanh^2(c_1 e_1)\right). \tag{14}$$

The Lyapunov function of this step is constructed as

$$V_1 = \frac{1}{2} e_1^2. \tag{15}$$

By invoking (12) and (13), the time derivative of (15) satisfies

$$\dot{V}_1 = -\mathcal{K} e_1 \tanh(c_1 e_1) - \frac{V_M}{r} f(\theta_M) e_1 e_2, \tag{16}$$

where $\mathcal{K} = k_a V_M f(\theta_M)/r$.

Step 2: Differentiating (11) with respect to time and substituting (7) into it yield

$$\dot{e}_2 = \frac{a_M}{V_M} + \frac{\Delta a_M}{V_M} - \frac{g\cos\gamma_M}{V_M} - \dot{\lambda} - \dot{\theta}_d, \tag{17}$$

where $\Delta a_M = \text{sat}(a_M) - a_M$, which denotes the differences between the guidance commands with saturation treatment and the guidance commands to be designed.

Now the control input, i.e., the guidance law in this paper, is selected as

$$a_M = \frac{V_M\left(k_b^2 - \theta_M^2\right)}{k_b^2}\left(-c_2 e_2 + \frac{V_M}{r} f(\theta_M) e_1 + \chi\right) + V_M\left(\frac{k_b^2 - \theta_M^2}{k_b^2}\dot{\theta}_d \varrho(e_2, \theta_d) + \frac{g\cos\gamma_M}{V_M} + \dot{\lambda}\right), \tag{18}$$

where c_2 is a positive constant, and

$$\varrho(e_2, \theta_d) = \frac{k_b}{2e_2} \ln \frac{(k_b + e_2 + \theta_d)(k_b - \theta_d)}{(k_b - e_2 - \theta_d)(k_b + \theta_d)}. \tag{19}$$

It can be shown, using L'Hôpital's rule, that

$$\lim_{e_2 \to 0} \varrho(e_2, \theta_d) = \lim_{e_2 \to 0} \frac{k_b^2}{k_b^2 - (e_2 + \theta_d)^2} = \frac{k_b^2}{k_b^2 - \theta_d^2}, \tag{20}$$

so we know that $\varrho(e_2, \theta_d)$ is bounded when $e_2 \to 0$ by applying $|\theta_d| < k_b$ from Property 2 and (13).

In addition, the variable χ in guidance law (18), utilized to compensate the effect of input saturation, is designed as the output of a first-order auxiliary filter, which is given by

$$\dot{\chi} = -\frac{1}{\tau}\chi + \frac{\Delta a_M}{V_M}, \quad \chi(t_0) = 0, \tag{21}$$

and

$$\frac{1}{\tau} = c_3 + \frac{\frac{2k_b^2 |e_2 \Delta a_M|}{V_M |k_b^2 - \theta_M^2|} + \frac{\Delta a_M^2}{V_M^2}}{2\chi^2 + S(\chi)}, \tag{22}$$

where c_3 is a positive constant and the switching function $S(\chi)$ is given by

$$S(\chi) = \begin{cases} 1, & \chi = 0, \\ 0, & \chi \neq 0. \end{cases} \tag{23}$$

It can be known from (21) that the variable χ will not stay at zero if the input saturation occurs. Whereas $\chi \equiv 0$ if the saturation treatment on the guidance command is never in effect.

The iBLF for this step can be constructed as

$$\begin{aligned} V_2 &= \int_0^{e_2} \frac{\sigma k_b^2}{k_b^2 - (\sigma + \theta_d)^2} d\sigma \\ &= \frac{k_b^2}{2} \ln \frac{k_b^2 - \theta_d^2}{k_b^2 - (e_2 + \theta_d)^2} \\ &\quad + \frac{k_b \theta_d}{2} \ln \frac{(k_b - e_2 - \theta_d)(k_b + \theta_d)}{(k_b + e_2 + \theta_d)(k_b - \theta_d)}. \end{aligned} \tag{24}$$

By using the results in [42], it can be obtained that V_2 is positive definite with respect to e_2 on $|\theta_M| < k_b$.

Differentiating (24) with respect to time yields

$$\dot{V}_2 = \frac{k_b^2 e_2 \dot{e}_2}{k_b^2 - \theta_M^2} + \left(\frac{k_b^2}{k_b^2 - \theta_M^2} - \varrho(e_2, \theta_d)\right) e_2 \dot{\theta}_d. \tag{25}$$

Substituting (17) and (18) into (25) and utilizing Young's inequality result in

$$\begin{aligned}\dot{V}_2 &= -c_2 e_2^2 + \frac{V_M}{r} f(\theta_M) e_1 e_2 + e_2 \chi + \frac{k_b^2 e_2 \Delta a_M}{V_M \left(k_b^2 - \theta_M^2\right)} \\ &\leq -\left(c_2 - \frac{1}{2}\right) e_2^2 + \frac{1}{2}\chi^2 + \frac{V_M}{r} f(\theta_M) e_1 e_2 \\ &\quad + \frac{k_b^2 |e_2 \Delta a_M|}{V_M \left|k_b^2 - \theta_M^2\right|}. \end{aligned} \tag{26}$$

In addition, another Lyapunov function for this step can be chosen as

$$V_3 = \frac{1}{2}\chi^2. \tag{27}$$

If the input saturation occurs during the interception, i.e., if the variable $\chi \neq 0$, by invoking (21) and (22) and using Young's inequality, the time derivative of (27) satisfies

$$\begin{aligned}\dot{V}_3 &= -c_3 \chi^2 - \frac{k_b^2 |e_2 \Delta a_M|}{V_M \left|k_b^2 - \theta_M^2\right|} - \frac{\Delta a_M^2}{2V_M^2} + \frac{\Delta a_M \chi}{V_M} \\ &\leq -\left(c_3 - \frac{1}{2}\right) \chi^2 - \frac{k_b^2 |e_2 \Delta a_M|}{V_M \left|k_b^2 - \theta_M^2\right|}. \end{aligned} \tag{28}$$

Then the performances of missile under the proposed guidance law are to be analyzed theoretically in the next subsection.

C. ANALYSIS OF THE GUIDANCE LAW

The guidance objectives with multiple constraints for the missile under the guidance law (18) can all be achieved via the proof of the following theorem.

Theorem 1: The guidance law (18) can guarantee homing constraint, impact angle control and seeker's FOV limit simultaneously for a missile intercepting a stationary target.

Proof. (1) Seeker's FOV limit. The Lyapunov function of the guidance system is selected as

$$V = V_1 + V_2 + V_3. \tag{29}$$

In the case $\chi \neq 0$, differentiating (29) with respect to time and substituting (16), (26) and (28) into it yield

$$\dot{V} \leq -\mathcal{K} e_1 \tanh(c_1 e_1) - \left(c_2 - \frac{1}{2}\right) e_2^2 - (c_3 - 1)\chi^2. \tag{30}$$

And in the case $\chi = 0$, it can be verified that (30) also holds. According to Assumption 1, 2, Lemma 1 and Property 1, we know that the $\dot{V}(t)$ is negative semidefinite with respect to the vector $[e_1, e_2, \chi]^T$, i.e., $\dot{V}(t) \leq 0$, by selecting $c_2 > 1/2$ and $c_3 > 1$. Then using Assumption 3, Property 2, (11), (13) and (24) results in the existence and boundedness of $V_2(t_0)$, which further lead to the existence and boundedness of $V(t_0)$ by combining (10), (15), (21), (27) and (29). Thus, we have $V(t) \leq V(t_0)$ on $t \geq t_0$, which further results in the boundedness of $V(t)$. Assume that there exists some time $t = t_1 > t_0$ such that $|\theta_M(t_1)| = k_b$, then $V(t_1)$ becomes unbounded from (11), (24) and (29), contradicting the boundedness of $V(t)$. As a conclusion, $\forall t \geq t_0$, we have $|\theta_M(t)| \neq k_b$, and the inequality $|\theta_M(t)| < k_b$ always holds since $\theta_M(t)$ is a continuous function with initial condition $|\theta_M(t_0)| < k_b$ in Assumption 3, so the target is always within the seeker's FOV with the proposed guidance law.

(2) Impact angle control. It can be obtained from Corollary 1 that $\mathcal{K} > 0$ during the guidance since $|\theta_M(t)| < k_b$ on $t \geq t_0$ has been proved. According ro Property 1, we have $\dot{V}(t)$ is negative definite with respect to the vector $[e_1, e_2, \chi]^T$, so e_1 and e_2 converge to zero, i.e. λ converges to $-\gamma_d$ from (10). Thus, the impact angle control can be guaranteed by the proposed guidance scheme.

(3) Homing constraint. On the one hand, it is known from (11) that θ_M converges to θ_d as e_2 converges to zero under the proposed guidance law. Then from (13), we have θ_M converges to zero ultimately since θ_d converges to zero as e_1 converges to zero. On the other hand, it can be obtained from (2), Assumption 1 and the inequality $|\theta_M(t)| < k_b$ that $\dot{r} < 0$ always holds during the interception, which shows that the homing constraint is not violated by the proposed guidance strategy, and this is the end of this proof.

Remark 1: When the missile is equipped with a passive sensor such as an infrared seeker or a passive sonar, the range information is difficult to measure in real time. To settle this problem, the relative range between missile and target, r, in guidance law (18) can be replaced with $-V_M \sin\theta_M / \dot{\lambda}$ according to (3).

IV. NUMERICAL SIMULATIONS

In this section, the performance of the proposed guidance law is demonstrated via four subsections involving numerical simulations. Let $t_0 = 0$, and to model the boost phase with fuel-injection at the initial stage, the missile thrust and mass are considered as

$$T = \begin{cases} 33000, & 0 \leq t < 1.5 \text{ s}, \\ 7500, & 1.5 \text{ s} \leq t < 8.5 \text{ s}, \\ 0, & t \geq 8.5 \text{ s}, \end{cases} \tag{31}$$

$$m = \begin{cases} 135 - 14.53t, & 0 \leq t < 1.5 \text{ s}, \\ 113.205 - 3.31t, & 1.5 \text{ s} \leq t < 8.5 \text{ s}, \\ 90.035, & t \geq 8.5 \text{ s}. \end{cases} \tag{32}$$

The drag is modeled as

$$D = C_{D0} Q S_{ref} + \frac{K_i m^2 a^2}{Q S_{ref}}, \tag{33}$$

where $a = \text{sat}(a_M)$, and C_{D0}, K_i, Q and S_{ref} denote the zero-lift drag coefficient, included drag coefficient, dynamic pressure and reference area respectively. The exact values and expressions of these parameters were given in [47].

A. ALL-ASPECT IMPACTS

This subsection shows the performances of missiles under the proposed guidance law against a stationary target with different impact angles. The initial conditions of the missiles are selected as follows. The missiles are launched at $(0, 0)$ with initial flight path angles $\gamma_M(0) = 50$ deg and initial

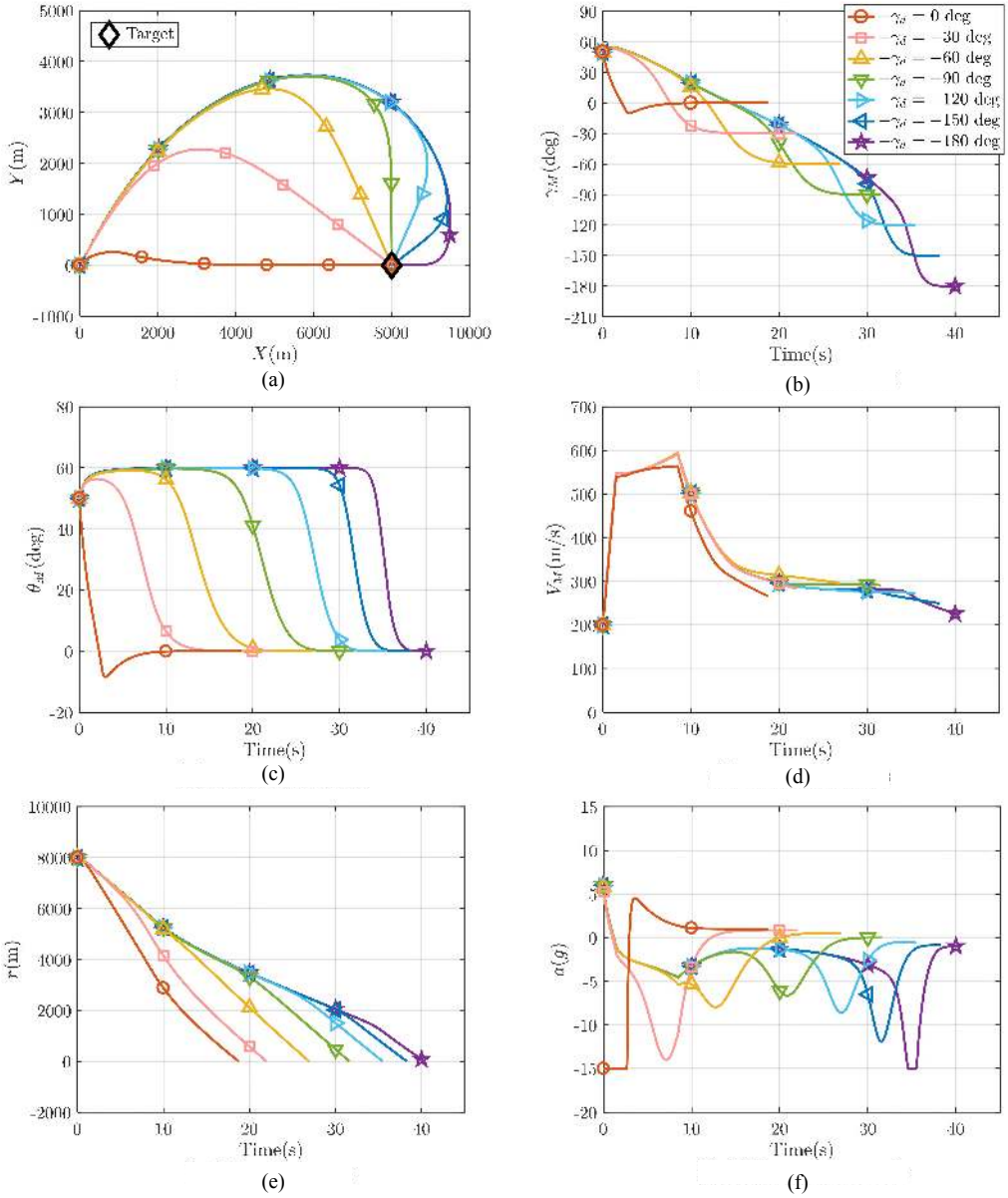

FIGURE 2. Simulation results of Subsection IV-A. (a) Flight trajectories. (b) Flight path angles. (c) Missile lead angles. (d) Missile velocities. (e) Relative ranges. (f) Guidance commands.

velocities V_M (0) = 200 m/s. The target is fixed at (8000, 0). The maximum seeker FOV value is set as 60 deg. The upper bound of the guidance commands $a_{\max}$ is selected as $15g$, where $g = 9.8$ m/s^2. And the parameters in the proposed guidance law is chosen as $c_1 = 5$, $c_2 = 5$, $c_3 = 10$, and $\varepsilon = 0.001$.

The simulation results of these scenarios are presented in Fig. 2. It is seen from Fig. 2(a) that the missiles intercept the target with impact angles from 0 deg to -180 deg successfully, and the flight path angles converge to the desired values before the interception in Fig. 2(b), which demonstrate the all-aspect interception capability of the missiles with the proposed guidance strategy. The missile lead angles in Fig. 2(c) never exceed the prescribed value to maintain the seekers lock-on. Meanwhile, the homing constraints are guaranteed by the convergence of missile lead angles in Fig. 2(c) and the decrease of the relative ranges in Fig. 2(e). Besides, the guidance commands plotted in Fig. 2(f) are always continuous and within the maximum limit during the whole interception.

Furthermore, we also notice the following two key points of the simulation results in Fig. 2. Firstly, It takes more time for a missile to achieve a larger desired impact angle (we consider the absolute value of the angle here), as shown in Fig. 2(e). In fact, the missile flight path angles in Fig. 2(b) cannot converge to their desired values with arbitrary short time, because it must be time consuming for a missile to fly over some distance, and then rotate its velocity vector towards the target from a desired direction with bounded missile velocity value. Secondly, It takes the minimum efforts for the missile to achieve the interception with the impact

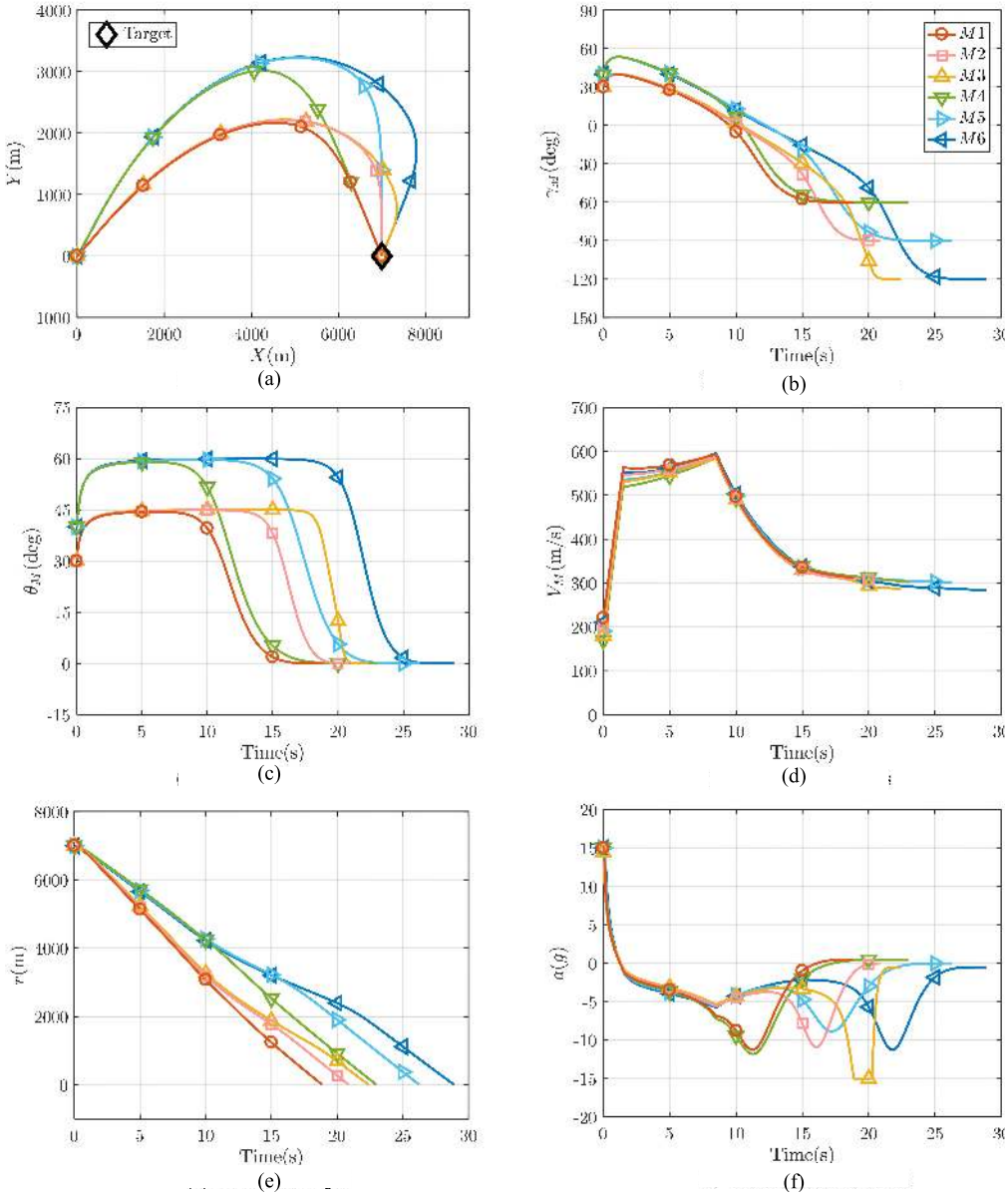

FIGURE 3. Simulation results of Subsection IV-B. (a) Flight trajectories. (b) Flight path angles. (c) Missile lead angles. (d) Missile velocities. (e) Relative ranges. (f) Guidance commands.

angle -90 deg, and the missile acceleration reaches a larger value with an impact angle which is smaller of larger than -90 deg in Fig. 2(f). And we can see from Fig. 2(a) that the missile trajectory with the impact angle -90 deg is the least curved in the seven profiles.

B. IMPACTS WITH DIFFERENT INITIAL CONDITIONS AND FOV RANGES

This subsection demonstrates the proposed guidance law with different initial conditions and FOV ranges. Assume that six missiles are launched at $(0, 0)$ and the target is fixed at $(7000, 0)$. The initial conditions, desired impact angles and maximum FOV limits are listed in TABLE 1. The upper bound of the guidance commands and the parameters in the proposed law are set as same as that in Subsection IV-A.

TABLE 1. Simulation settings for subsection IV-B.

Missile	$M1$	$M2$	$M3$	$M4$	$M5$	$M6$
Desired impact angle (deg)	-60	-90	-120	-60	-90	-120
Initial flight path angle (deg)	30	30	30	40	40	40
Initial missile velocity (m/s)	220	200	180	170	190	210
Maximum FOV limit (deg)	45	45	45	60	60	60

The simulation results of these cases are plotted in Fig. 3. It can be obtained from Fig. 3 that the missiles in these six different scenarios achieve the interceptions with desired impact angles successfully, and the missile lead angles and the guidance commands are within their prescribed limit values respectively. In addition, the following two aspects can be obtained from the simulation results. Firstly, it is seen from Fig. 3(e) that the guidance processes with smaller lead angle limits are more time saving, since the absolute values

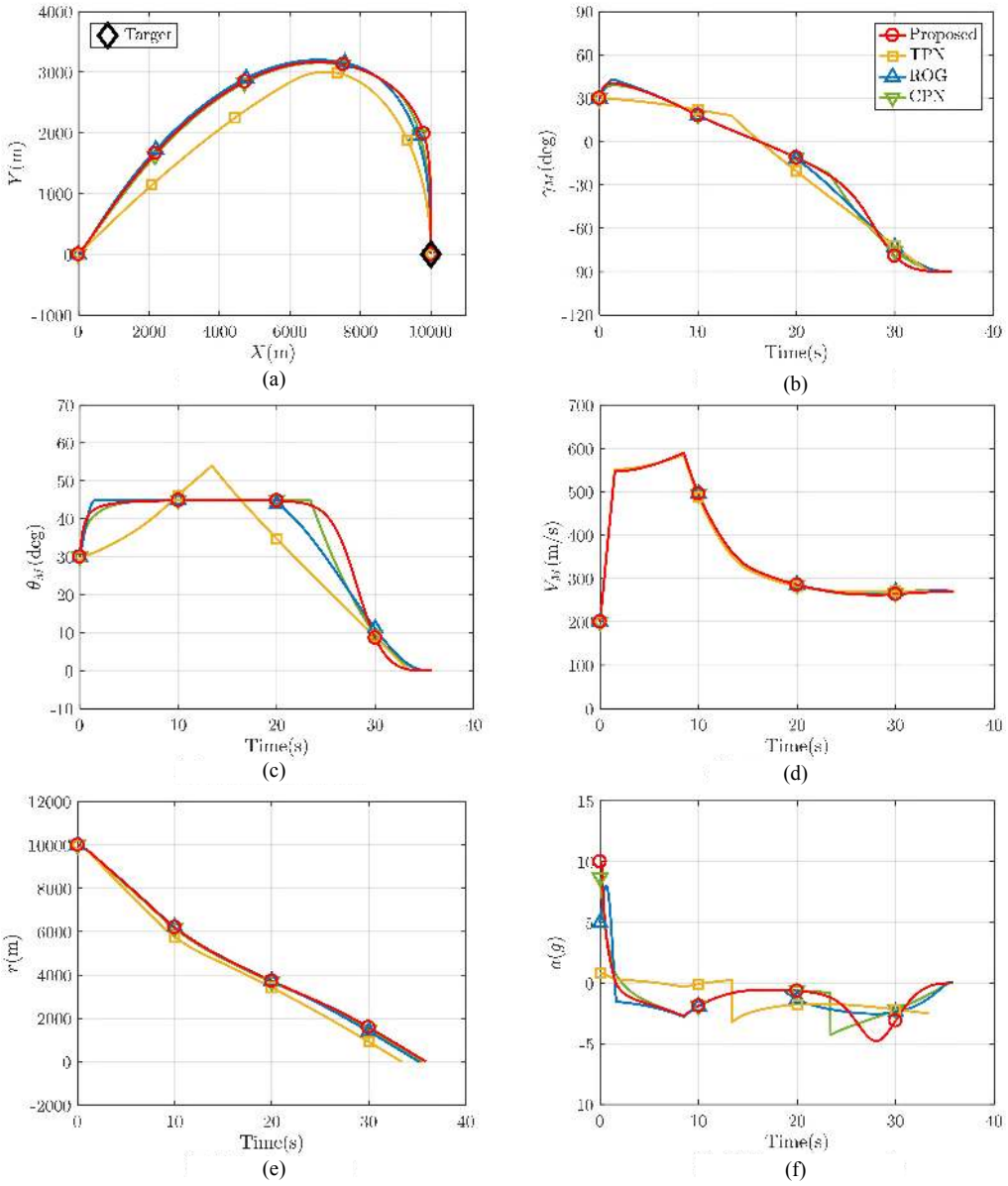

FIGURE 4. Simulation results of Subsection IV-C. (a) Flight trajectories. (b) Flight path angles. (c) Missile lead angles. (d) Missile velocities. (e) Relative ranges. (f) Guidance commands.

of the relative velocities between missile and target, i.e., $|\dot{r}|$, become larger with smaller lead angles in (2). Secondly, It seems that the missile prefers to achieve the interception with a lead angle as large as possible with the proposed law in Fig. 3(c), though it results in a longer flight trajectory and longer guidance time as in Fig. 3(a) and (e). As a result, it is ascertained that the task of FOV constrained IACG in these different scenarios can be carried out for the missiles with the proposed guidance law.

C. COMPARISONS WITH OTHER ADVANCED GUIDANCE LAWS

For the advantage analysis of the proposed guidance law, the missile performances under the proposed method are compared with three typical advanced guidance strategies, which are two-stage proportional navigation (TPN) [11], range-to-go weighted optimal guidance (ROG) [32], and composite proportional navigation (CPN) [37], respectively.

TPN is the classic two-phase guidance strategy for impact angle control but free for seeker's FOV limit. We summarize the expression of TPN as

$$a_{\mathrm{TPN}} = \begin{cases} \dfrac{2}{\pi}\gamma_M(0)\, V_M \dot{\lambda}, & \dfrac{\gamma_d - \gamma_M}{\gamma_d - \lambda} < 2, \\ N_1 V_M \dot{\lambda}, & \dfrac{\gamma_d - \gamma_M}{\gamma_d - \lambda} = 2, \end{cases} \tag{34}$$

where $N_1 = 2$. Besides, ROG is the representative of FOV constrained IACG law derived based on linear method, and it

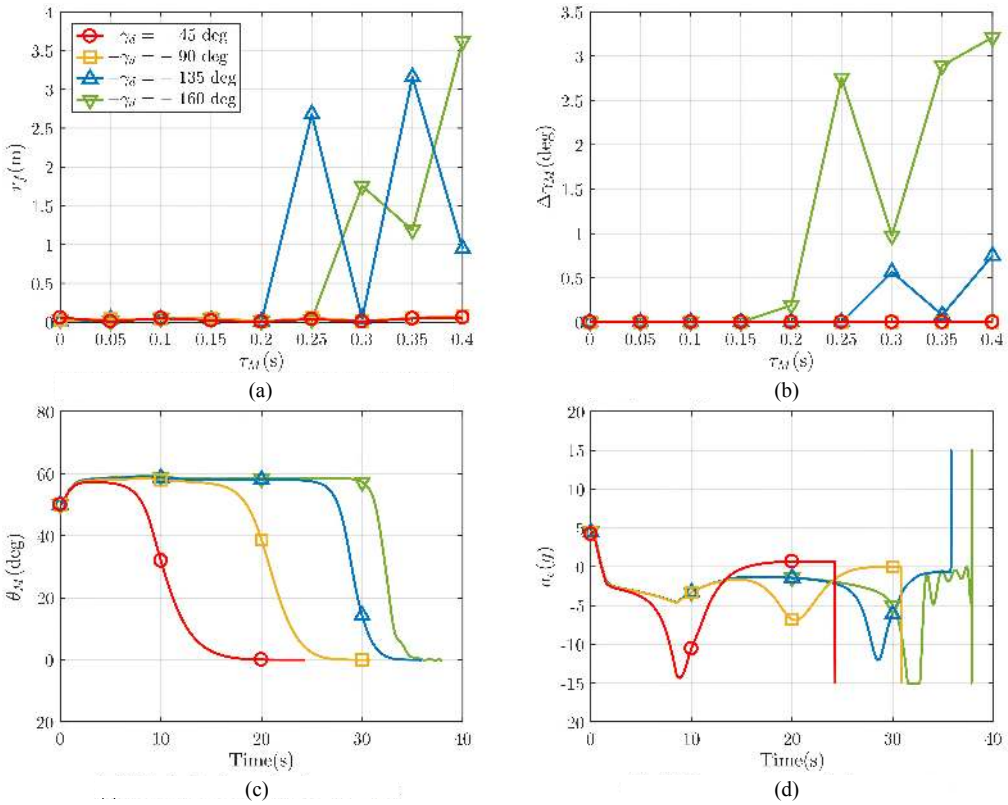

FIGURE 5. Simulation results of Subsection IV-D. (a) Miss distances for various time constants. (b) Impact angle error for various constants. (c) Missile lead angles for $\tau_M = 0.3$. (d) Guidance commands for $\tau_M = 0.3$.

is given by

$$a_{\mathrm{ROG}} = \begin{cases} -(N_2+3)\,V_M^2\left(\dfrac{r\theta_M - k_b r_1}{r^{N_2+3} - r_1^{N_2+3}}\right) r^{N_2+1} \\ \quad + \dfrac{\mu r^{N_2}}{V_M^2}\left(1 - \left(\dfrac{N_2+3}{N_2+2}\right)\left(\dfrac{r^{N_2+2} - r_1^{N_2+2}}{r^{N_2+3} - r_1^{N_2+3}}\right)\right), \\ \qquad\qquad r_1 < r < r\,(0)\,, \\ V_M\dot{\lambda}, \qquad\qquad r_2 < r < r_1, \\ -\dfrac{V_M^2}{r}\left((N_2+2)\,(N_2+3)\,\theta_M\right. \\ \quad \left. + (N_2+1)\,(N_2+2)\,(\gamma_d - \gamma_M)\right), \\ \qquad\qquad 0 < r < r_2, \end{cases} \tag{35}$$

where $N_2 = 1$, the values of μ, r_1 and r_2 are determined in [32]. Then CPN, the representative of PN based approach, is excerpted as

$$a_{\mathrm{CPN}} = \begin{cases} V_M\dot{\lambda} + K\,(k_b - \theta_M)\,, & |\lambda| < |\lambda_s|\,, \\ N_3 V_M\dot{\lambda}, & |\lambda| \geq |\lambda_s|\,, \end{cases} \tag{36}$$

where $N_3 = 3$, $K = 300$, and λ_s is defined in [37].

In this subsection, it is assumed that the missiles under four different guidance laws are launched at (0, 0) with initial flight path angles 30 deg and initial velocities $V_M\,(0) = 200$ m/s. The target is fixed at (10000, 0). The desired impact angle $-\gamma_d$ is selected as -90 deg and the maximum seeker FOV value is set as 45 deg. The upper bound of guidance commands is set as $10g$ and the parameters in the proposed method is chosen as same as that in Subsection IV-A.

TABLE 2. Performance summary for subsection IV-C.

Guidance law	Impact time	Miss distance	Impact angle error
Proposed	35.83 s	0.0994 m	$< 10^{-4}$ deg
TPN	33.41 s	0.2476 m	0.0024 deg
ROG	35.17 s	0.0584 m	$< 10^{-4}$ deg
CPN	35.43 s	0.0146 m	0.0010 deg

The performance summary of the four guidance laws in these scenarios at the final time is given in TABLE 2, and the simulation results are shown in Fig. 4. It is seen from TABLE 2 that all of the four missiles with different guidance laws impact the target with both small impact angle errors and acceptable miss distances. Fig 4(a) shows that the missiles trajectories under ROG, CPN and the proposed law are similar. The missile lead angle under TPN exceeds the prescribed limit in Fig. 4(c), since FOV constraint is not considered in its design. In Fig. 4(f), the guidance commands under CPN jump down when the missile lead angle leaves the maximum value in Fig. 4(c). In Fig. 4(f), the guidance commands under ROG and the proposed guidance law are always continuous, but the implementation of ROG needs the calculations of the transient values μ, r_1 and r_2, where numerical computation processes are involved to solve complex nonlinear equations.

In addition, the guidance commands under the proposed law in Fig. 4(f) are less than that under ROG and CPN in the short time before interception, which indicates that the missile with the proposed law takes the lead to achieve the desired impact angle and the impact condition ($\theta_M \to 0$), as shown in Fig. 4(b) and (c). Therefore, the proposed guidance law shows better performances compared with other three advanced laws.

D. FIRST-ORDER LAG SYSTEM CONSIDERATION

In this subsection, the simulations for a realistic missile model with first order autopilot lag are conducted. The autopilot dynamics is given by

$$\frac{a_M}{a_c} = \frac{1}{\tau_M s + 1}, \tag{37}$$

where a_c denotes the commands generated by guidance computer, the time constants τ_M varies from 0 to 0.4 s. And the impact angles -45 deg, -90 deg, -135 deg and -160 deg are considered here. The parameter ε is set as 0.1 and the simulation scenario and other parameter selections are set as same as that in Subsection IV-A.

The value of ε in this subsection is selected larger than that in the former three subsections, since the missile autopilot dynamics (37) is not modeled in guidance system (7), the tracking error e_2 under the commands a_c may increase due to this lag effect. According to (11) and (13), in order to ensure that the missile lead angle does not exceed the prescribed limit value, the range of θ_d should be reduced appropriately, i.e., the value of ε should be somewhat enlarged.

The miss distances (r_f) and impact angle errors ($\Delta\gamma_M$) with different time constants are summarized in Fig. 5(a) and (b), respectively. And the profiles of missile lead angles and guidance commands for $\tau_M = 0.3$ s are shown in Fig. 5(c) and (d), respectively. We noticed that the guidance precision with impact angles -45 deg and -90 deg are almost unaffected with the varying of the time constants. However, the miss distances and impact angle errors become large for $\tau_M > 0.25$ s with the desired impact angles of -135 deg as well as -160 deg, and they reach their maximums 3.6226 m and 3.2109 deg respectively for $\tau_M = 0.4$ s. From Fig. 5(c) and (d), we know that though the guidance commands diverge at the final guidance time, the missile lead angle are always within the allowable range and converge to the small neighborhood of zero eventually to guarantee the impact. The results describe the applicability of the proposed law in the realistic missile model.

V. CONCLUSION

A novel nonlinear and non-switching FOV constrained IACG strategy is proposed in this paper for a missile attacking a stationary target. A new nonlinear control oriented mathematical model with time-varying missile velocity consideration is established. Hyperbolic tangent function is used in the first step to design a bounded virtual guidance law. The effect of the input saturation is compensated in the second step with a first-order filter. IBLF based stability analysis shows that the tracking errors of the guidance system converge to zero uniformly, and the prescribed guidance constraints can be guaranteed simultaneously. Numerical simulations demonstrate that the missiles can achieve the interceptions successfully with all rational aspects and many different specified conditions, which illustrate the effectiveness of the proposed law.

REFERENCES

[1] P. Zarchan, *Tactical and Strategic Missile Guidance*, 6th ed. Washington, DC, USA: AIAA, 2012.
[2] M. Kim and K. V. Grider, "Terminal guidance for impact attitude angle constrained flight trajectories," *IEEE Trans. Aerosp. Electron. Syst.*, vol. AES-9, no. 6, pp. 852–859, Nov. 1973.
[3] C.-K. Ryoo, H. Cho, and M.-J. Tahk, "Optimal guidance laws with terminal impact angle constraint," *J. Guid., Control, Dyn.*, vol. 28, no. 4, pp. 724–732, 2005.
[4] C.-K. Ryoo, H. Cho, and M.-J. Tahk, "Time-to-go weighted optimal guidance with impact angle constraints," *IEEE Trans. Control Syst. Technol.*, vol. 14, no. 3, pp. 483–492, May 2006.
[5] A. Ratnoo and D. Ghose, "State-dependent Riccati-equation-based guidance law for impact-angle-constrained trajectories," *J. Guid., Control, Dyn.*, vol. 32, no. 1, pp. 320–326, 2009.
[6] Y. I. Lee, S. H. Kim, and M.-J. Tahk, "Optimality of linear time-varying guidance for impact angle control," *IEEE Trans. Aerosp. Electron. Syst.*, vol. 48, no. 4, pp. 2802–2817, Oct. 2012.
[7] C.-H. Lee, M.-J. Tahk, and J.-I. Lee, "Generalized formulation of weighted optimal guidance laws with impact angle constraint," *IEEE Trans. Aerosp. Electron. Syst.*, vol. 49, no. 2, pp. 1317–1322, Apr. 2013.
[8] R. Bardhan and D. Ghose, "Nonlinear differential games-based impact-angle-constrained guidance law," *J. Guid., Control Dyn.*, vol. 38, no. 3, pp. 384–402, Feb. 2015.
[9] C.-H. Lee and M.-G. Seo, "New insights into guidance laws with terminal angle constraints," *J. Guid., Control Dyn.*, vol. 41, no. 8, pp. 1832–1837, Aug. 2018.
[10] P. Lu, D. B. Doman, and J. D. Schierman, "Adaptive terminal guidance for hypervelocity impact in specified direction," *J. Guid., Control, Dyn.*, vol. 29, no. 2, pp. 269–278, Mar. 2006.
[11] A. Ratnoo and D. Ghose, "Impact angle constrained interception of stationary targets," *J. Guid., Control, Dyn.*, vol. 31, no. 6, pp. 1816–1821, Nov. 2008.
[12] A. Ratnoo and D. Ghose, "Impact angle constrained guidance against nonstationary nonmaneuvering targets," *J. Guid., Control, Dyn.*, vol. 33, no. 1, pp. 269–275, Jan. 2010.
[13] K. S. Erer and O. Merttopçuoglu, "Indirect impact-angle-control against stationary targets using biased pure proportional navigation," *J. Guid., Control, Dyn.*, vol. 35, no. 2, pp. 700–704, 2012.
[14] C. H. Lee, T. H. Kim, and M. J. Tahk, "Interception angle control guidance using proportional navigation with error feedback," *J. Guid., Control, Dyn.*, vol. 36, no. 5, pp. 1556–1561, Sep. 2013.
[15] S. Ghosh, D. Ghose, and S. Raha, "Composite guidance for impact angle control against higher speed targets," *J. Guid., Control Dyn.*, vol. 39, no. 1, pp. 98–117, Jan. 2016.
[16] S. R. Kumar, S. Rao, and D. Ghose, "Sliding-mode guidance and control for all-aspect interceptors with terminal angle constraints," *J. Guid., Control, Dyn.*, vol. 35, no. 4, pp. 1230–1246, 2012.
[17] S. Rao and D. Ghose, "Terminal impact angle constrained guidance laws using variable structure systems theory," *IEEE Trans. Control Syst. Technol.*, vol. 21, no. 6, pp. 2350–2359, Nov. 2013.
[18] S. Xiong, W. Wang, X. Liu, S. Wang, and Z. Chen, "Guidance law against maneuvering targets with intercept angle constraint," *ISA Trans.*, vol. 53, no. 4, pp. 1332–1342, Jul. 2014.
[19] S. R. Kumar, S. Rao, and D. Ghose, "Nonsingular terminal sliding mode guidance with impact angle constraints," *J. Guid., Control, Dyn.*, vol. 37, no. 4, pp. 1114–1130, 2014.
[20] Y. Zhao, Y. Sheng, and X. Liu, "Sliding mode control based guidance law with impact angle constraint," *Chin. J. Aeronaut.*, vol. 27, no. 1, pp. 145–152, Feb. 2014.
[21] Y. Zhao, Y. Sheng, and X. Liu, "Impact angle constrained guidance for all-aspect interception with function-based finite-time sliding mode control," *Nonlinear Dyn.*, vol. 85, no. 3, pp. 1791–1804, Aug. 2016.

[22] Z. Hou, L. Liu, Y. Wang, J. Huang, and H. Fan, "Terminal impact angle constraint guidance with dual sliding surfaces and model-free target acceleration estimator," *IEEE Trans. Control Syst. Technol.*, vol. 25, no. 1, pp. 85–100, Jan. 2017.
[23] D. Cho, H. J. Kim, and M.-J. Tahk, "Impact angle constrained sliding mode guidance against maneuvering target with unknown acceleration," *IEEE Trans. Aerosp. Electron. Syst.*, vol. 51, no. 2, pp. 1310–1323, Apr. 2015.
[24] S. He, W. Wang, and D. Lin, "Adaptive backstepping impact angle guidance law accounting for autopilot lag," *J. Aerosp. Eng.*, vol. 30, no. 3, May 2017, Art. no. 04016094.
[25] S. He, W. Wang, and J. Wang, "Adaptive backstepping impact angle control with autopilot dynamics and acceleration saturation consideration," *Int. J. Robust Nonlinear Control*, vol. 27, no. 17, pp. 3777–3793, Nov. 2017.
[26] S. He, T. Song, and D. Lin, "Impact angle constrained integrated guidance and control for maneuvering target interception," *J. Guid., Control Dyn.*, vol. 40, no. 10, pp. 2652–2660, Oct. 2017.
[27] Z. Cheng, L. Liu, and Y. Wang, "Lyapunov-based switched-gain impact angle control guidance," *Chin. J. Aeronaut.*, vol. 31, no. 4, pp. 765–775, Apr. 2018.
[28] M.-G. Seo, C.-H. Lee, and M.-J. Tahk, "New design methodology for impact angle control guidance for various missile and target motions," *IEEE Trans. Control Syst. Technol*, vol. 26, no. 6, pp. 2190–2197, Nov. 2018.
[29] C. H. Lee, T. H. Kim, M. J. Tahk, and I. H. Whang, "Polynomial guidance laws considering terminal impact angle and acceleration constraints," *IEEE Trans. Aerosp. Electron. Syst.*, vol. 49, no. 1, pp. 74–92, Jan. 2013.
[30] T. H. Kim, C. H. Lee, and M. J. Tahk, "Time-to-go polynomial guidance with trajectory modulation for observability enhancement," *IEEE Trans. Aerosp. Electron. Syst.*, vol. 49, no. 1, pp. 55–73, Jan. 2013.
[31] B.-G. Park, T.-H. Kim, and M.-J. Tahk, "Optimal impact angle control guidance law considering the seeker's field-of-view limits," *Proc. Inst. Mech. Eng., G, J. Aerosp. Eng.*, vol. 227, no. 8, pp. 1347–1364, Jun. 2013.
[32] B.-G. Park, T.-H. Kim, and M.-J. Tahk, "Range-to-go weighted optimal guidance with impact angle constraint and seeker's look angle limits," *IEEE Trans. Aerosp. Electron. Syst.*, vol. 52, no. 3, pp. 1241–1256, Jun. 2016.
[33] T.-H. Kim, B.-G. Park, and M.-J. Tahk, "Bias-shaping method for biased proportional navigation with terminal-angle constraint," *J. Guid., Control Dyn.*, vol. 36, no. 6, pp. 1810–1816, Nov. 2013.
[34] B.-G. Park, T.-H. Kim, and M.-J. Tahk, "Biased PNG with terminal-angle constraint for intercepting nonmaneuvering targets under physical constraints," *IEEE Trans. Aerosp. Electron. Syst.*, vol. 53, no. 3, pp. 1562–1572, Jun. 2017.
[35] R. Tekin and K. S. Erer, "Switched-gain guidance for impact angle control under physical constraints," *J. Guid., Control Dyn.*, vol. 38, no. 2, pp. 205–216, Feb. 2015.
[36] A. Ratnoo, "Analysis of two-stage proportional navigation with heading constraints," *J. Guid., Control Dyn.*, vol. 39, no. 1, pp. 156–164, Jan. 2016.
[37] B.-G. Park, H.-H. Kwon, Y.-H. Kim, and T.-H. Kim, "Composite guidance scheme for impact angle control against a nonmaneuvering moving target," *J. Guid., Control Dyn.*, vol. 39, no. 5, pp. 1129–1136, May 2016.
[38] S. He and D. Lin, "A robust impact angle constraint guidance law with seeker's field-of-view limit," *Trans. Inst. Meas. Control*, vol. 37, no. 3, pp. 317–328, Mar. 2015.
[39] X. Wang, Y. Zhang, and H. Wu, "Sliding mode control based impact angle control guidance considering the seeker's field-of-view constraint," *ISA Trans.*, vol. 61, pp. 49–59, Mar. 2016.
[40] H.-G. Kim, J.-Y. Lee, and H.-J. Kim, "Look angle constrained impact angle control guidance law for homing missiles with bearings-only measurements," *IEEE Trans. Aerosp. Electron. Syst*, vol. 54, no. 6, pp. 3096–3107, Dec. 2018.
[41] Y. Zhang, X. Wang, and H. Wu, "Impact time control guidance with field-of-view constraint accounting for uncertain system lag," *Proc. Inst. Mech. Eng., G, J. Aerosp. Eng.*, vol. 230, no. 3, pp. 515–529, Mar. 2016.
[42] K. P. Tee and S. S. Ge, "Control of state-constrained nonlinear systems using integral Barrier Lyapunov functionals," in *Proc. IEEE 51st Conf. Decis. Control (CDC)*, Maui, HI, USA, Dec. 2012, pp. 3239–3244.
[43] Z.-L. Tang, S. S. Ge, K. P. Tee, and W. He, "Robust adaptive neural tracking control for a class of perturbed uncertain nonlinear systems with state constraints," *IEEE Trans. Syst., Man, Syst.*, vol. 46, no. 12, pp. 1618–1629, Dec. 2016.
[44] Y.-J. Liu, J. Li, S. Tong, and C. L. P. Chen, "Neural network control-based adaptive learning design for nonlinear systems with full-state constraints," *IEEE Trans. Neural Netw. Learn. Syst.*, vol. 27, no. 7, pp. 1562–1571, Jul. 2016.
[45] D. Zhou and B. Xu, "Adaptive dynamic surface guidance law with input saturation constraint and autopilot dynamics," *J. Guid., Control Dyn.*, vol. 39, no. 5, pp. 1152–1159, May 2016.
[46] S. Xiong, M. Wei, M. Zhao, X. Hua, W. Wang, and B. Zhou, "Hyperbolic tangent function weighted optimal intercept angle guidance law," *Aerosp. Sci. Technol.*, vol. 78, pp. 604–619, Jul. 2018.
[47] P. Kee, D. Li, and S. Chai, "Near optimal midcourse guidance law for flight vehicle," in *Proc. 36th Aiaa Aerosp. Sci. Meeting Exhib.*, Reno, NV, USA, 1998, pp. 1–11.

BOJUN LIU (S'18) received the B.Eng. degree in automation from Northwestern Polytechnical University, Xi'an, China, in 2016, where he is currently pursuing the Ph.D. degree in control science and engineering. His research interests include missile guidance and control, and nonlinear control systems.

MINGSHAN HOU received the B.Eng. degree in flight control, and the M.Eng. and Ph.D. degrees in navigation, guidance and control from Northwestern Polytechnical University, Xi'an, China, in 1983, 1986, and 1989, respectively, where he is currently a Professor. His research interests include missile guidance, flight control, robust control, and modeling and optimization of complex systems.

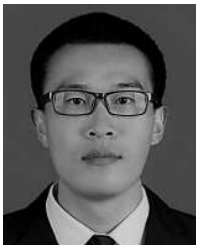

YAJUN LI received the B.Eng. degree in electrical engineering and automation from Harbin Engineering University, Harbin, China, in 2014. He is currently pursuing the Ph.D. degree in control science and engineering with the Northwestern Polytechnical University, Xi'an, China. His research interests include hypersonic flight control and nonlinear control systems.